Whole-Body Biodistribution and Estimation of Radiation-Absorbed Doses of the Dopamine D_1 Receptor Radioligand ^{11}C-NNC 112 in Humans

Vanessa L. Cropley, BSc[1]; Masahiro Fujita, MD, PhD[1]; John L. Musachio, PhD[1]; Jinsoo Hong, MS[1]; Subroto Ghose, MD, PhD[1]; Janet Sangare, C-RNP[1]; Pradeep J. Nathan, PhD[2]; Victor W. Pike, PhD[1]; and Robert B. Innis, MD; PhD[1]

[1]*Molecular Imaging Branch, National Institute of Mental Health, National Institutes of Health, Bethesda, Maryland; and* [2]*Department of Physiology, Monash Centre for Brain and Behaviour, Monash University, Clayton, Victoria, Australia*

The present study estimated radiation-absorbed doses of the dopamine D_1 receptor radioligand [^{11}C](+)-8-chloro-5-(7-benzofuranyl)-7-hydroxy-3-methyl-2,3,4,5-tetrahydro-1*H*-3-benzazepine) (NNC 112) in humans, based on dynamic whole-body PET in healthy subjects. **Methods:** Whole-body PET was performed on 7 subjects after injection of 710 ± 85 MBq of ^{11}C-NNC 112. Fourteen frames were acquired for a total of 120 min in 7 segments of the body. Regions of interest were drawn on compressed planar images of source organs that could be identified. Radiation dose estimates were calculated from organ residence times using the OLINDA 1.0 program. **Results:** The organs with the highest radiation-absorbed doses were the gallbladder, liver, lungs, kidneys, and urinary bladder wall. Biexponential fitting of mean bladder activity demonstrated that 15% of activity was excreted via the urine. With a 2.4-h voiding interval, the effective dose was 5.7 μSv/MBq (21.1 mrem/mCi). **Conclusion:** ^{11}C-NNC 112 displays a favorable radiation dose profile in humans and would allow multiple PET examinations per year to be performed on the same subject.

Key Words: ^{11}C-NNC 112; PET; D_1 receptor; dosimetry; effective dose

J Nucl Med 2006; 47:100–104

Abnormalities in dopamine have been implicated in several psychiatric and neurodegenerative disorders such as schizophrenia, Parkinson's disease, attention deficit hyperactivity disorder, and drug dependence. Dopamine D_1 receptors are highly distributed in the brain, with the highest density being found in the striatum and regions of the basal ganglia, followed by such regions of the cerebral cortex as the prefrontal cortex, thalamus, hippocampus, and amygdala (*1,2*). D_1 receptors in the brain have been implicated in the regulation of motor and cognitive activity such as locomotor behavior, working memory, and executive functions (*3–5*).

[^{11}C](+)-8-Chloro-5-(7-benzofuranyl)-7-hydroxy-3-methyl-2,3,4,5-tetrahydro-1*H*-3-benzazepine) (NNC 112) is2 a high-affinity (dissociation constant, 0.18 nmol/L) dopamine D_1 receptor radioligand that can image low-density D_1 receptors in striatal and extrastriatal regions. ^{11}C-NNC 112 displays higher specific-to-nonspecific ratios than does an older, commonly used ligand, ^{11}C-SCH-23390 (*6,7*), and is highly reliable for PET quantification (*7*). Radiation-absorbed dose estimates of ^{11}C-NNC 112 have not been reported; therefore, the present study was performed to obtain human dosimetry estimates of ^{11}C-NNC 112 based on serial whole-body PET scans of healthy subjects.

MATERIALS AND METHODS

Radiopharmaceutical Preparation

The (+)-desmethyl NNC 112 (*6*) (1.0 mg per radiolabeling) was obtained from Professor Christer Halldin of the Karolinska Institutet. ^{11}C-NNC 112, originally reported by Halldin et al. (*6*), was synthesized in radiolabeled form from ^{11}C-methyl iodide via a captive solvent method using a commercially available radiochemistry "loop" module. The radiochemical purity of all the ^{11}C-NNC 112 syntheses was greater than 99%, with an average specific activity of 47.0 ± 12.58 GBq/μmol (1.27 ± 0.34 Ci/μmol).

Subjects

The study was approved by the Radiation Safety Committee of the National Institutes of Health and the Institutional Review Board of the National Institute of Mental Health. Seven healthy volunteers (4 male and 3 female; mean age ± SD, 28 ± 8 y; range, 21–42 y) participated in the study. All subjects were free of current medical and psychiatric illness based on history, a physical examination, routine laboratory tests (including a complete blood count, chemistries, urinalysis, urine drug screening, and HIV and hepatitis B tests), and an electrocardiogram. Furthermore, after completion of the PET scan, standard screening laboratory tests were repeated on every subject.

Received Aug. 4, 2005; revision accepted Oct. 7, 2005.
For correspondence or reprints contact: Vanessa L. Cropley, BSc, Molecular Imaging Branch, NIMH, National Institute of Health, Bldg. 1, Room B3-10, 1 Center Dr., MSC 0135, Bethesda, MD 20892-0135.
E-mail: cropleyv@mail.nih.gov

PET Data Acquisition

Subjects underwent transmission and dynamic emission scans on an Advance tomograph (GE Healthcare). Before tracer injection, transmission scans using ^{68}Ge rods were obtained on 7 segments of 15 cm each (the axial field of view of the Advance scanner) from the head to the upper thigh to permit measured attenuation correction. The duration of each transmission was 3 min. After intravenous bolus administration of 710 ± 85 MBq (19 ± 2 mCi) of ^{11}C-NNC 112, dynamic emission scans of 14 frames were acquired by serial imaging of the body in the 7 contiguous segments. The duration of initial frames was 15 s at each segment, followed by frames of increasing length, with six 3-s intervals to move the bed to the next section and 13 s to move the bed back to the first bed position. The total scanning time approximated 120 min (4 × 0.25, 3 × 0.5, 3 × 1, 3 × 2, and 1 × 4 min for each of 7 body sections from head to mid thigh).

The tomographic PET images were compressed into a single anterior-posterior planar image. Planar images were analyzed instead of tomographic images to facilitate visualization of organs. A previous study in our laboratory (*8*) demonstrated that analysis of compressed planar images is comparable to that of tomographic images, but with a slight overestimation (i.e., conservative calculation) of organ radiation burden. Images were analyzed using pixelwise modeling computer software (PMOD 2.55; PMOD Group) on the compressed planar images. Regions of interest were drawn on source organs that could be identified. Large regions of interest were drawn to ensure that all accumulated radioactivity, which consisted of both parent and metabolite radioactivities, in each organ was encompassed. The "remainder of body" was calculated for each time point as the decayed value of all activity in the segment minus activity in the identified source organs.

Residence Time Calculation

At each time point, decayed data of the identified source organs were converted to the fraction of the injected dose by dividing the organ activities by the total injected activity and plotted versus time. The total injected activity was calculated as the entire activity in frame 1 in each of the 7 segments. Time–activity curves (percentage injected dose [%ID] vs. time) for the source organs were created. The area under the time–activity curve for each organ was calculated by the trapezoidal method up to the last data acquisition at 120 min. To be conservative, we calculated the area under the curve from the last data acquisition to infinity by assuming that the decline in radioactivity occurred by only physical decay, without any further biologic clearance. The area under the time–activity curve of source organ from time zero to infinity is equivalent to residence time (h).

Organ Absorbed Dose

The activity overlying the bladder represented the total urinary excretion during the scanning interval. For each subject, decay-corrected cumulative urine activity was fitted with a biexponential curve by limiting the urine activity to no more than 100% of the injected activity, and the total excretion in urine in terms of %ID and biologic half-life was determined. The dynamic bladder model (*9*) implemented in OLINDA/EXM version 1.0 (*10*) was used to calculate the residence time of the urinary bladder wall with urine-voiding intervals of 2.4 and 4.8 h. Organ absorbed doses were based on the OLINDA/EXM scheme of a 70-kg man, using the residence time of the source organs calculated above.

RESULTS

The injection of ^{11}C-NNC 112 caused no significant change in heart rate or blood pressure, and no significant effects were observed in blood or urine tests performed approximately 5–30 min after termination of the scan. After injection of ^{11}C-NNC 112, the brain, lungs, liver, heart, spleen, kidneys, small intestine, gallbladder, and urinary bladder were visually identified as organs with moderate to high activity in most subjects (Fig. 1). However, the heart was not visualized in 4 subjects, and the small intestine was not visualized in 2 subjects. For the heart and small intestine, the average time–activity curve and residence time were based on 3 and 5 subjects, respectively. Uptake of ^{11}C-NNC 112 was highest in the lungs, with a peak of 28 %ID occurring at the first frame acquisition. Peak values of the %ID to the liver, brain, heart, kidneys, small intestine, and gallbladder were 22, 7, 5, 4, 4, and 1.4, respectively, and all occurred within 5 min. Figure 2 demonstrates the time–activity curves of the source organs at the average time that they were imaged.

The accumulated activity over the bladder was fitted with a biexponential curve to estimate the fraction of injected activity excreted via this route (Fig. 3). In some cases, the fitting of the biexponential curve did not converge; in these instances, the first 1 or 2 data points were eliminated because there were relatively high activities in surrounding soft tissue, compared with that in the urinary bladder. After this step, the biexponential curve well described the accumulation of radioactivity over the bladder, with a mean r^2 value of 0.999. According to this fit, the average fraction excreted via urine was approximately 15%, and biologic half-lives were 0.04 and 1.5 h. In most subjects, at the end of the study, the small intestine showed decay-corrected activity of 9.7 %ID. Because of the short half-life, the rest of the injected activity would have decayed before excretion to the bladder or intestine.

The average residence times for the 7 subjects are shown in Figure 4. From the organ residence times and the percentage of activity excreted via the urine, radiation-absorbed dose was estimated for each subject, with urine-voiding

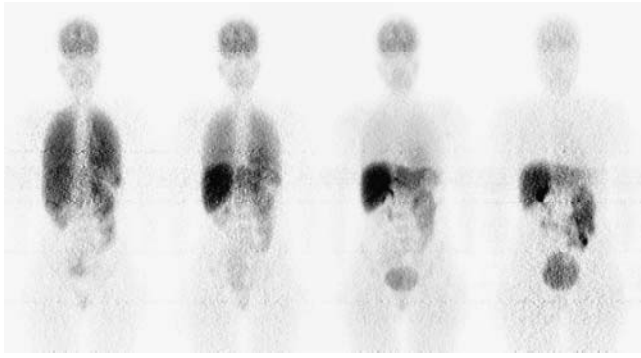

FIGURE 1. Compressed anteroposterior whole-body planar images showing distribution of radioactivity in representative healthy subject at approximately 1, 5, 22, and 90 min after ^{11}C-NNC 112 injection.

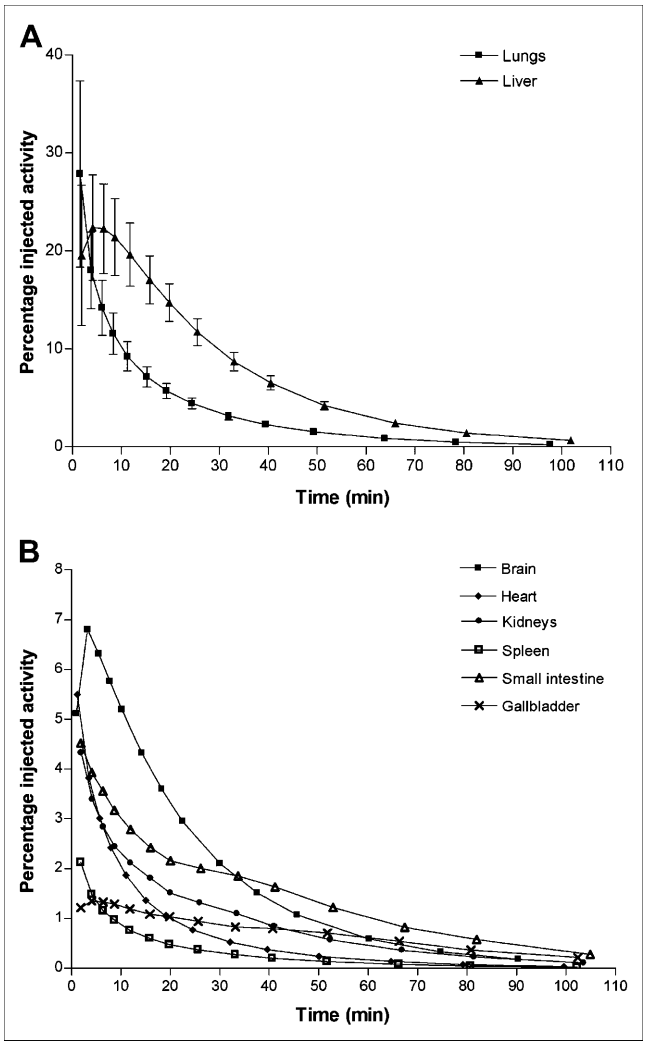

FIGURE 2. (A) Time–activity curves for ^{11}C-NNC 112 serial PET of lungs and liver. Data are expressed as mean ± SD of 7 subjects and are not corrected for radioactive decay. (B) Time–activity curves for ^{11}C-NNC 112 serial PET of 6 organs. Data are expressed as average of 7 subjects for brain, kidneys, spleen, and gallbladder; average of 5 subjects for small intestine; and average of 3 subjects for heart and are not corrected for radioactive decay. For clarity, SD error bars are not included.

intervals of 2.4 and 4.8 h. There was only a 2% difference in the dose to the urinary bladder wall at urine-voiding intervals of 2.4 and 4.8 h. The effective doses were 5.71 and 5.77 μSv/MBq, with 2.4- and 4.8-h voiding intervals, respectively. With a 2.4-h voiding interval, the organs with the highest radiation burden (μSv/MBq) were the gallbladder (32.4), followed by the liver (22.2), lungs (16.9), kidneys (16.6), and urinary bladder wall (15.7). Table 1 summarizes organ absorbed dose estimates for humans.

DISCUSSION

In the present study, serial whole-body ^{11}C-NNC 112 PET studies were performed on healthy humans to estimate radiation-absorbed doses of ^{11}C-NNC 112. Whole-body

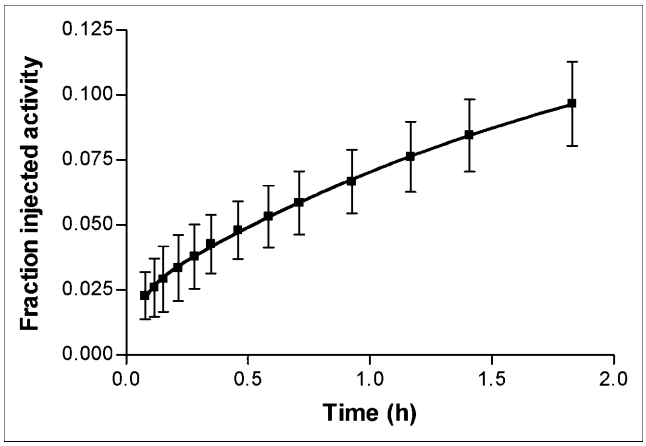

FIGURE 3. Decay-corrected cumulative urinary excretion of radioactivity after injection of ^{11}C-NNC 112. Data reflect mean ± SD bladder activity measured by PET in 7 subjects. Solid line reflects biexponential fitting of average bladder activity with PRISM software (version 4.0). Two-phase exponential association was used, defined as $Y = Ymax1 \times (1 - \exp(-K1 \times X)) + Ymax2 \times (1 - \exp(-K2 \times X))$, where Y = cumulative urinary excretion, Ymax1 and Ymax2 = 2 fractions of urinary excretion at the infinite time, X = h, and K1 and K2 = rate constants. Urine activity was constrained to not exceed 100% of injected activity (Ymax1 + Ymax2 ≤ 1), and half-times were defined as ln(2)/K1 and ln(2)/K2. Asymptote of curve indicates that approximately 15 %ID was excreted via urine. Fitting to biexponential curve yielded half-lives of 0.04 and 1.5 h.

imaging of ^{11}C-NNC 112 revealed that this D_1 receptor radioligand caused only modest radiation exposure, with an effective dose of 5.7 μSv/MBq. With injected activities of 523–788 MBq (14–22 mCi), which are frequently used in brain-imaging studies, this effective dose of 5.7 μSv/MBq (21.1 mrem/mCi) would yield an effective dose of 2.98–4.49 mSv (0.29–0.46 rem). This would allow multiple PET

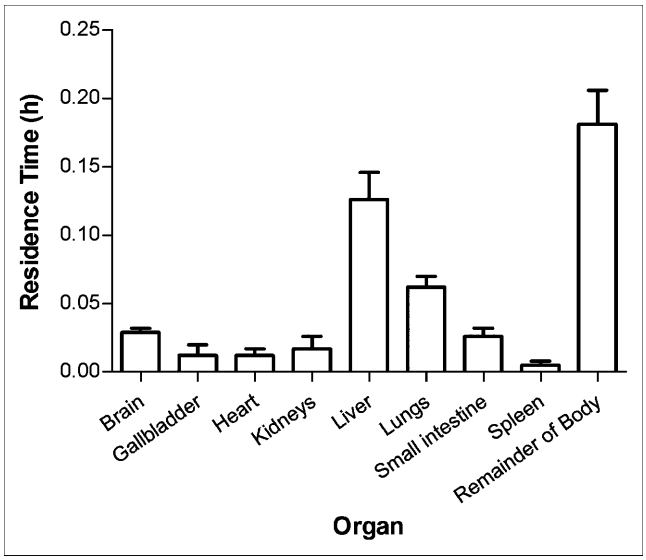

FIGURE 4. For 7 subjects, average residence times (h) calculated from whole-body planar images of ^{11}C-NNC 112. Values are mean ± SD.

TABLE 1
Radiation Dose Estimates of ^{11}C-NNC 112

Target organ	μGy/MBq	mrad/mCi
Adrenals	3.5	13.0
Brain	6.9	25.6
Breasts	1.7	6.2
Gallbladder wall	32.4	120.0
Lower large intestine wall	2.0	7.3
Small intestine	7.5	27.8
Stomach	2.3	8.6
Upper large intestine wall	3.0	11.0
Heart wall	6.6	24.4
Kidneys	16.6	61.4
Liver	22.2	82.1
Lungs	16.9	62.6
Muscle	1.8	6.5
Ovaries	2.2	8.2
Pancreas	3.4	12.6
Red marrow	1.9	6.9
Bone surfaces	2.2	8.3
Skin	1.3	4.6
Spleen	9.4	35.0
Testes	1.3	4.9
Thymus	1.9	7.1
Thyroid	1.5	5.4
Urinary bladder wall	15.7	58.1
Uterus	2.5	9.3
Total body	2.8	10.3

Dynamic urinary bladder model was used, based on 2.4-h void. Effective dose equivalent = 9.2 μSv/MBq (33.9 mrem/mCi). Effective dose = 5.7 μSv/MBq (21.1 mrem/mCi).

studies per year to be performed on the same subject. Furthermore, the absence of effects on vital signs (heart rate and blood pressure) or on standard blood and urine tests after ^{11}C-NNC 112 injection indicate that ^{11}C-NNC 112 is also safe from a pharmacologic perspective.

The present study demonstrated that the gallbladder is the organ with the highest radiation burden (32.4 μSv/MBq), followed by the liver, lungs, and kidneys. Because planar images were used instead of tomographic images to improve visualization of organs, the gallbladder activities are likely to have included liver activities, and the dose to the gallbladder may have been overestimated. Because planar images were analyzed and large regions of interest were drawn, the present study may have, in general, slightly overestimated the radiation exposure of source organs, resulting in conservative estimates of organ radiation burden. High uptake of ^{11}C-NNC 112 (peak uptake, 28 %ID) initially occurred in the lungs, contributing to the relatively high radiation burden to this organ. This high activity in the lungs at early times reflects distribution of ^{11}C-NNC 112, although the clearance of ^{11}C-NNC 112 from the lungs was rapid, decreasing to 50% of its peak value within 8 min after injection, based on non–decay-corrected data. Activity from injected ^{11}C-NNC 112 at later times primarily reflects elimination of the tracer via the gastrointestinal and urinary routes. Because the distribution of radioactivity in peripheral organs does not match that of dopamine D_1 receptors, and because ^{11}C-NNC 112 was metabolized quickly, most of the activities detected in peripheral organs in this study were likely from radioactive metabolites not binding to the receptor. Biexponential fitting of bladder activity demonstrated that only 15% of total activity was excreted via urine. Although there may be errors in the parameter estimation for the urinary excretion because of the short data acquisition, the impact on dose estimations with a 2.4-h urine interval should be minimal because the data were acquired for 2 h—that is, 83% of the interval. Although uptake of ^{11}C-NNC 112 reached a maximum within 5–10 min for all source organs, clearance of ^{11}C-NNC 112 from the liver, gallbladder, and small intestine was quite slow. In most subjects, at the end of the study, the small intestine showed decayed-corrected activity of 9.7 %ID. Because of the short half-life of ^{11}C (20.4 min), the rest of the injected activity (~75%) would have decayed before excretion to the bladder or intestine.

The short half-life of ^{11}C also raises the question of whether human biodistribution studies of ^{11}C-labeled ligands need to be performed, provided that radiation dose estimates in rodents or nonhuman primates have been completed. Table 2 displays effective dose estimates of ^{11}C-labeled ligands obtained from biodistribution studies on humans. For all the tracers listed in Table 2, the estimated effective dose is quite low, allowing multiple injections of the tracer per year in the same subject. With the exception of 1 study (*11*), which resulted in a conservative estimation of overall radiation burden from ^{11}C-WAY 100635, the effective dose of the ^{11}C tracers shows modest variation, ranging from 4.3 to 7.0 μSv/MBq. With inclusion of ^{11}C-WAY 100635, the effective dose varies appreciably by a factor of 3.3. This relatively large discrepancy may be due to actual differences in radiation exposure from the different ^{11}C-labeled tracers or, rather, may reflect differences in study design and analysis of data.

TABLE 2
Comparison of Radiation Burden of ^{11}C-NNC 112 with Other ^{11}C-Labeled Radioligands in Humans

Radioligand	Effective dose (μSv/MBq)	Reference
^{11}C-WAY100635	14.1	*11*
^{11}C-Raclopride	6.7	*12*
^{11}C-DASB	7.0	*13*
^{11}C-Glucose	4.3	*14*
^{11}C-Methionine	5.2	*15*
^{11}C-Methoxyprogabidic acid	4.8	*16*
^{11}C-Acetate	4.9	*17*
^{11}C-Flumazenil	5.0	*18*
^{11}C-Mirtazapine	6.8	*19*
^{11}C-Raclopride	6.5	*20*
^{11}C-NNC 112	5.7	—

CONCLUSION

The dopamine D_1 receptor radioligand ^{11}C-NNC 112 appears to be safe for humans, yielding a relatively modest radiation burden that would permit multiple PET studies per year to be performed on the same subject.

ACKNOWLEDGMENTS

We gratefully acknowledge Peter Herscovitch (chief) and the staff of the PET department for the successful completion of the study. We thank Cyrill Burger, PhD, Piotr Rudnicki, PhD, Krzysztof Mikolajczyk, PhD, and Michal Grodzki, PhD, for providing the PMOD 2.55 software and Jeih-San Liow, PhD, for technical assistance. This research was supported (in part) by the Intramural Research Program of the National Institutes of Health and National Institute of Mental Health.

REFERENCES

1. Hall H, Sedvall G, Magnusson O, et al. Distribution of D_1 and D_2-dopamine receptors, and dopamine and its metabolites in the human brain. *Neuropsychopharmacology.* 1994;11:245–256.
2. Meador-Woodruff JH, Damask SP, Wang J, et al. Dopamine receptor mRNA expression in human striatum and neocortex. *Neuropsychopharmacology.* 1996;15:17–29.
3. Centonze D, Grande C, Saulle E, et al. Distinct roles of D_1 and D_5 dopamine receptors in motor activity and striatal synaptic plasticity. *J Neurosci.* 2003;23:8506–8512.
4. Sawaguchi T, Goldman-Rakic PS. The role of D_1-dopamine receptor in working memory: local injections of dopamine antagonists into the prefrontal cortex of rhesus monkeys performing an oculomotor delayed response task. *J Neurophysiol.* 1994;71:515–528.
5. Vallone D, Picetti R, Borrelli E. Structure and function of dopamine receptors. *Neurosci Biobehav Rev.* 2000;24:125–132.
6. Halldin C, Foged C, Chou YH, et al. Carbon-11-NNC 112: a radioligand for PET examination of striatal and neocortical D_1-dopamine receptors. *J Nucl Med.* 1998;39:2061–2068.
7. Abi-Dargham A, Martinez D, Mawlawi O, et al. Measurement of striatal and extrastriatal dopamine D_1 receptor binding potential with [^{11}C]NNC 112 in humans: validation and reproducibility. *J Cereb Blood Flow Metab.* 2000; 20:225–243.
8. Tipre DN, Lu JQ, Fujita M, et al. Radiation dosimetry estimates for the PET serotonin transporter probe [^{11}C]DASB determined from whole-body imaging in nonhuman primates. *Nucl Med Commun.* 2004;25:81–86.
9. Cloutier RJ, Smith SA, Watson EE, et al. Dose to the fetus from radionuclides in the bladder. *Health Phys.* 1973;25:147–161.
10. Stabin M, Sparks GRB, Crowe E. OLINDA/EXM: the second generation personal computer software for internal dose assessment in nuclear medicine. *J Nucl Med.* 2005;46:1023–1027.
11. Parsey R, Belanger VMJ, Sullivan GM, et al. Biodistribution and radiation dosimetry of ^{11}C-WAY100,635 in humans. *J Nucl Med.* 2005;46:614–619.
12. Ribeiro MJ, Ricard M, Bourgeois S, et al. Biodistribution and radiation dosimetry of [^{11}C]raclopride in healthy volunteers. *Eur J Nucl Med Mol Imaging.* 2005;32:952–958.
13. Lu JQ, Ichise M, Liow JS, et al. Biodistribution and radiation dosimetry of the serotonin transporter ligand ^{11}C-DASB determined from human whole-body PET. *J Nucl Med.* 2004;45:1555–1559.
14. Graham MM, Peterson LM, Muzi M, et al. 1-[Carbon-11]-glucose radiation dosimetry and distribution in human imaging studies. *J Nucl Med.* 1998; 39:1805–1810.
15. Deloar HM, Fujiwara T, Nakamura T, et al. Estimation of internal absorbed dose of L-[methyl-^{11}C]methionine using whole-body positron emission tomography. *Eur J Nucl Med.* 1998;25:629–633.
16. Santens P, De Vos F, Thierens H, et al. Biodistribution and dosimetry of carbon 11-methoxyprogabidic acid, a possible ligand for GABA-receptors in the brain. *J Nucl Med.* 1998;39:307–310.
17. Seltzer MA, Jahan SA, Sparks R, et al. Radiation dose estimates in humans for (^{11}C)acetate whole-body PET. *J Nucl Med.* 2004;45:1233–1236.
18. Nugent AC, Neumeister A, Drevets WC, et al. Human biodistribution and dosimetry of the PET benzodiazepine receptor radioligand [^{11}C]flumazenil [abstract]. *J Nucl Med.* 2004;45(suppl):434P.
19. Marthi K, Hansen SB, Jakobsen S, et al. Biodistribution and radiation dosimetry of [*N-methyl*-^{11}C]mirtazapine, an antidepressant affecting adrenoceptors. *Appl Radiat Isot.* 2003;59:175–179.
20. Slifstein M, Martinez D, Ekelund J, et al. Biodistribution and radiation dosimetry of the dopamine D_2 ligand [^{11}C]raclopride determined from human whole body PET [abstract]. *J Nucl Med.* 2005;46(suppl 2):343P.

JNM The Journal of NUCLEAR MEDICINE

Whole-Body Biodistribution and Estimation of Radiation-Absorbed Doses of the Dopamine D_1 Receptor Radioligand ^{11}C-NNC 112 in Humans

Vanessa L. Cropley, Masahiro Fujita, John L. Musachio, Jinsoo Hong, Subroto Ghose, Janet Sangare, Pradeep J. Nathan, Victor W. Pike and Robert B. Innis

J Nucl Med. 2006;47:100-104.

The Journal of Nuclear Medicine is published monthly.
SNMMI | Society of Nuclear Medicine and Molecular Imaging
1850 Samuel Morse Drive, Reston, VA 20190.
(Print ISSN: 0161-5505, Online ISSN: 2159-662X)

SNMMI SOCIETY OF NUCLEAR MEDICINE AND MOLECULAR IMAGING